

Support information

Plasma induced grafting carboxymethyl cellulose on multiwalled carbon nanotubes for the removal of UO_2^{2+} from aqueous solution

Dadong Shao, Zhongqing Jiang, Xiangke Wang*, Jiaying Li, Yuedong Meng

Key Lab of Novel Thin Film Solar Cells, Institute of Plasma Physics, Chinese

Academy of Sciences, P.O. Box 1126, 230031, Hefei, P.R. China

Dadong Shao: shaodadong@126.com

Zhongqing Jiang: zhongqingjiang@hotmail.com

Xiangke Wang: xkwang@ipp.ac.cn

Jiaying Li: lijx@ipp.ac.cn

Yuedong Meng: ydmeng@ipp.ac.cn

*: Corresponding author. Phone: +86-551-5592788; Fax: +86-551-5591310; Email:

xkwang@ipp.ac.cn (X.K. Wang).

The Journal of Physical Chemistry

Supplemental Information, 13 Pages

List of Supplemental Information Contents

SI-1. Chemical Materials.....	P. S3
SI-2. Preparation of CMC solution.....	P. S3-4
SI-3. FT-IR, Raman, XRD, TGA-DTA, and SEM characterization.....	P. S4
SI-4. N ₂ -BET measurement of raw MWCNT and MWCNT-g-CMC	P. S5
SI-5. Proposed mechanism of MWCNT grafted with CMC	P. S5-6
SI-6. Sorption experiment procedure of UO ₂ ²⁺ on raw MWCNT and MWCNT-g-CMC	P. S6-7
SI-7. Relative proportion of species distribution of U(VI)	P. S7-9
SI-8. Effect of pH on sorption of UO ₂ ²⁺ on raw MWCNT and MWCNT-g-CMC	P. S9-11
SI-9. Effect of ionic strength on sorption of UO ₂ ²⁺ on MWCNT-g-CMC	P. S11-12
SI-10. Reference cited.....	P. S12-13

Prepared: Dec. 23, 2008

SI-1. Chemical Materials

The chemicals $\text{UO}_2(\text{NO}_3)_2 \cdot 6\text{H}_2\text{O}$, NaClO_4 , HClO_4 , HNO_3 , NaOH , and Arsenaze-III were purchased in analytical purity, and sodium carboxymethyl cellulose (CMC) was purchased in chemical purity. All chemicals used without any further purification in the experiments. All the solutions were prepared with Milli-Q water under ambient conditions.

MWCNT was prepared by using chemical vapor deposition (CVD) of acetylene in hydrogen flow at 760 °C using Ni-Fe as catalysts.¹ $\text{Fe}(\text{NO}_3)_2$ and $\text{Ni}(\text{NO}_3)_2$ were treated by sol-gel process and calcinations to get FeO and NiO and then deoxidized by H_2 to get Fe and Ni nanoparticles. MWCNT was added into 3 mol/L HNO_3 solution to remove the hemispherical caps of the nanotubes. The mixture of 2 g MWCNT and 400 mL 3 mol/L nitric acid was ultrasonically stirred for 24 h. The suspension was filtrated and then rinsed with deionized water until the pH of the suspension reached about 6 and then was dried at 80 °C. Thus prepared MWCNT was calcined at 450 °C for 24 hours to remove the amorphous carbon. The catalysts Ni and Fe in the treated MWCNT were measured by ICP-MS and the results show that Ni and Fe are less than 0.01% and 0.03 wt. %, respectively.

SI-2. Preparation of CMC solution

3.0 g CMC was added into 150 mL Milli-Q water in a 250 mL Pyrex beaker step by step under continuum stirring at 70 °C (controlled by thermocouple). The CMC solution was natural cooled to room temperature after CMC was dissolved in Milli-Q

water thoroughly. The cooled CMC solution and Milli-Q water rinsings were transferred into a 200 mL Pyrex volumetric flask, and then proper volume Milli-Q water was added into the Pyrex volumetric flask to the calibration line. The CMC solution in the Pyrex volumetric flask was shaken up well, and thus 1.50 g/L CMC solution was obtained.

SI-3. FT-IR spectra, Raman spectra, XRD, TGA-DTA, and SEM characterization

The Fourier transform infrared spectroscopy (FT-IR) measurements of raw MWCNT, MWCNT-g-CMC and CMC samples were mounted by using Perkin-Elmer 100 spectrometer in KBr pellet at room temperature.

The Raman spectra of raw MWCNT and MWCNT-g-CMC samples were mounted by using a LabRam HR Raman spectrometry, excitation at 514.5 nm by Ar⁺ laser.

The raw MWCNT and MWCNT-g-CMC samples were characterized by using X-ray diffraction (XRD) (Rigaku D/max) with Cu K α radiation at room temperature.

TGA-DTA measurements of raw MWCNT and MWCNT-g-CMC were examined by using a Shimadzu TGA-50 thermogravimetric analyzer from 25 to 800 °C at the heating rate of 10 °C/min with an air flow rate of 50 mL/min.

The scanning electron microscopy (SEM) images of raw MWCNT and MWCNT-g-CMC were obtained at 5.0 kV on a field emission scanning electron microscope (FEI Sirion 200 FEG SEM).

SI-4. N₂-BET measurement of raw MWCNT and MWCNT-g-CMC

According to N₂-BET measurements (Figure SI-1), the specific surface areas were 93.59 m²/g for raw MWCNT and 70.76 m²/g for MWCNT-g-CMC, respectively.

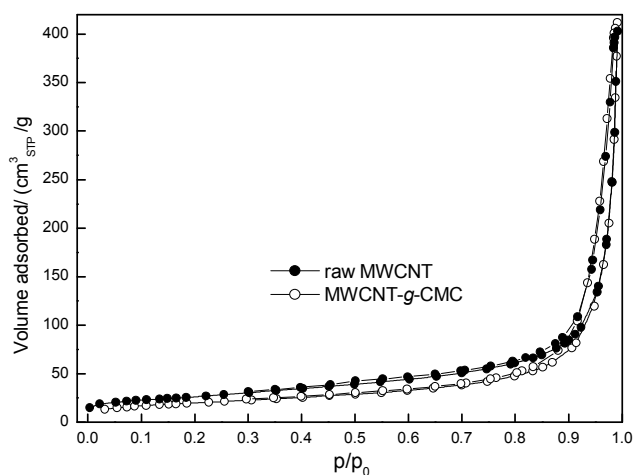


Figure SI-1. Adsorption-desorption isotherms of nitrogen gas on raw MWCNT and MWCNT-g-CMC

SI-5. Proposed grafting mechanism of MWCNT grafted with CMC

According FT-IR spectra, the -NH₂ vibration in MWCNT-treat and in MWCNT-g-CMC; and the hemiacetal vibration in MWCNT-g-CMC are found. The C2-C3 bond in the cellulose chain can be cleaved and forms hemiacetal.² It is well known, C-O-C band is weaker than C-C bond, the C-O-C band in cellulose can also be cleaved. The mechanism of MWCNT grafted with CMC induced by N₂ plasma is proposed and is shown in Figure SI-2.

Active nitrogen species (N^{*}) react with raw MWCNT to form -C-N^{*} at the defect position of MWCNT or replay the hydroxyl groups in N₂ plasma discharging process. The -C-N^{*} is converted to -C-NH₂ after plasma treatment, thus MWCNT treatment

material is obtained. $-C-N^*$ can react with CMC in the grafting process, and some glucose rings of CMC is broken. MWCNT grafted with CMC at the bond-broken position subsequently. It is reasonable that some of the bond-broken of CMC dose not take part in the grafting reaction with MWCNT, which forms hemiacetal, and some of the $-C-N^*$ might react with water molecule and is converted into $-C-NH_2$ groups.

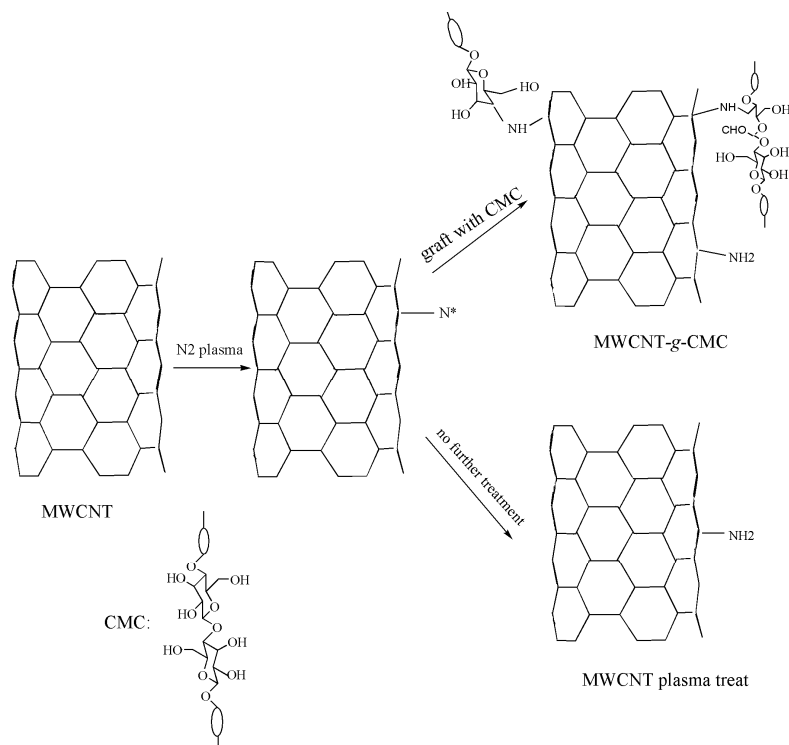


Figure SI-2. Proposed mechanism of MWCNT grafted with CMC

SI-6. Sorption experimental procedure of UO_2^{2+} on raw MWCNT and MWCNT-g-CMC

All the experiments were carried out at $T = 20 \pm 1$ °C. The stock solution of sorbents (2.40 g/L), $NaClO_4$ (6.00×10^{-2} mol/L) and UO_2^{2+} (1.20×10^{-4} mol/L) solution were added in the polyethylene test tubes to achieve the desired concentrations of different components. The pH values of the suspensions were adjusted to 5.0 ± 0.1 by adding

negligible volumes of 0.1 mol/L or 0.01 mol/L HClO₄ or NaOH. In the end, the suspension was purged with high-purity nitrogen gas to eliminate the effect of CO₂.

After the suspensions had been shaken for 24 h, the solid phase was separated from the liquid phase by centrifugation at 18000 rpm for 60 minutes, and then the supernatant was filtered using 0.45µm membrane filters.

The concentration of UO₂²⁺ was analyzed by Arsenazo III Spectrophotometric Method at wavelength of 650 nm. All the experimental data were the average of duplicate determinations, and the average uncertainties were < 5%.

The sorption percent (%) of UO₂²⁺ was calculated from the difference between the initial concentration (C₀) and the final concentration of UO₂²⁺ in the supernatant (C_{eq}):

$$\text{Sorption \%} = \frac{C_0 - C_{\text{eq}}}{C_0} \times 100\% \quad (1)$$

The concentration of UO₂²⁺ adsorbed on the solid phase (C_s) was calculated from the initial concentration (C₀), the final concentration (C_{eq}), the volume of the suspension (V) and the mass of the sorbent (m_{sorbent}):

$$C_s = \frac{C_0 - C_{\text{eq}}}{C_{\text{sorbent}}} = \frac{C_0 - C_{\text{eq}}}{m_{\text{sorbent}}} \times V \quad (2)$$

SI-7. Relative proportion of species distribution of U(VI)

In order to properly interpret the U(VI) sorption behavior, we calculated the aqueous speciation of U(VI) as a function of pH in the absence of sorbent according to the thermodynamic data listed in Table SI-1.³

Table SI-1. Aqueous complexation reactions of U(VI).³

Reactions	logK (I = 0)
$\text{UO}_2^{2+} + \text{H}_2\text{O} = \text{UO}_2(\text{OH})^+ + \text{H}^+$	-5.25
$\text{UO}_2^{2+} + 2\text{H}_2\text{O} = \text{UO}_2(\text{OH})_2^0 + 2\text{H}^+$	-12.15
$\text{UO}_2^{2+} + 3\text{H}_2\text{O} = \text{UO}_2(\text{OH})_3^- + 3\text{H}^+$	-20.25
$\text{UO}_2^{2+} + 4\text{H}_2\text{O} = \text{UO}_2(\text{OH})_4^{2-} + 4\text{H}^+$	-32.4
$2\text{UO}_2^{2+} + \text{H}_2\text{O} = (\text{UO}_2)_2(\text{OH})^{3+} + \text{H}^+$	-2.70
$2\text{UO}_2^{2+} + 2\text{H}_2\text{O} = (\text{UO}_2)_2(\text{OH})_2^{2+} + 2\text{H}^+$	-5.62
$3\text{UO}_2^{2+} + 5\text{H}_2\text{O} = (\text{UO}_2)_3(\text{OH})_5^+ + 5\text{H}^+$	-15.55
$3\text{UO}_2^{2+} + 7\text{H}_2\text{O} = (\text{UO}_2)_3(\text{OH})_7^- + 7\text{H}^+$	-32.20
$4\text{UO}_2^{2+} + 7\text{H}_2\text{O} = (\text{UO}_2)_4(\text{OH})_7^+ + 7\text{H}^+$	-21.90

The distribution of aqueous U(VI) species in water solution at different U(VI) concentrations (2.00×10^{-4} mol/L, 5.00×10^{-5} mol/L, 1.00×10^{-5} mol/L, and 1.00×10^{-6} mol/L) were given in Figure SI-3. As can be seen from Figure SI-3, the distribution of U(VI) species showed a dependency on pH values and U(VI) total concentration. Free uranyl ion (UO_2^{2+}) was the dominant species at $\text{pH} < 5$, and then U(VI) hydrolysis complexes, and multinuclear hydroxide complexes were the dominant species in 2.00×10^{-4} - 1.00×10^{-7} mol/L U(VI) aqueous solution. Furthermore, U(VI) species are positive charge in the pH range of ~5-8, and negative charge in the pH range above ~8 under experiment condition.

In the pH range of ~5-8, U(VI) species change gradually from multinuclear hydroxide complexes to hydroxide complexes with the decrease of U(VI) total concentration. $(\text{UO}_2)_3(\text{OH})_5^+$ and $(\text{UO}_2)_4(\text{OH})_7^+$ are the dominant specie in U(VI)

solution above 1.00×10^{-5} mol/L; whereas $\text{UO}_2(\text{OH})^+$ and $(\text{UO}_2)_3(\text{OH})_5^+$ are the dominant species in 1.00×10^{-6} mol/L U(VI) solution.

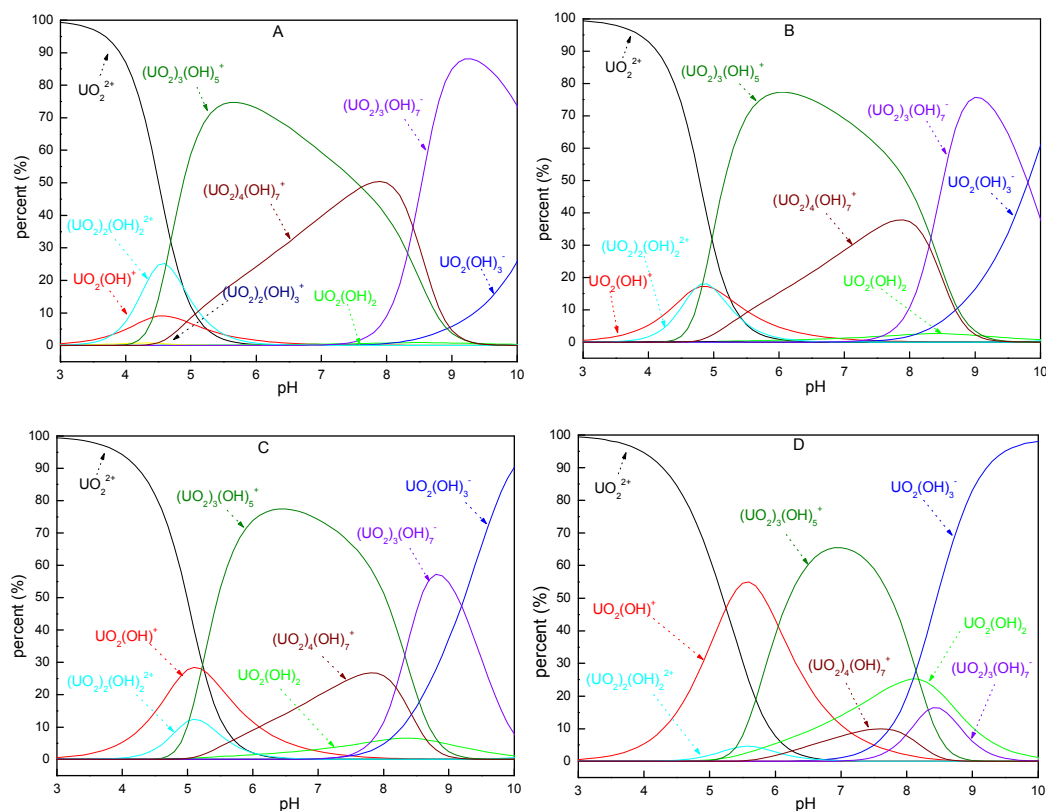


Figure SI-3. Distribution of aqueous U(VI) species. **Figure SI-3A:** $C[\text{U(VI)}]_{\text{total}} = 2.00 \times 10^{-4}$ mol/L; **Figure SI-3B:** $C[\text{U(VI)}]_{\text{total}} = 4.00 \times 10^{-5}$ mol/L; **Figure SI-3C:** $C[\text{U(VI)}]_{\text{total}} = 1.00 \times 10^{-5}$ mol/L; and **Figure SI-3D:** $C[\text{U(VI)}]_{\text{total}} = 1.00 \times 10^{-6}$ mol/L in water solution.

SI-8. Effect of pH on the sorption of UO_2^{2+} on raw MWCNT and MWCNT-g-CMC

The removal of UO_2^{2+} on raw MWCNT and on MWCNT-g-CMC as a function of pH was shown in Figure SI-4. As can be seen from Figure SI-4, the sorption percent of UO_2^{2+} on MWCNT-g-CMC increased rapidly from $\sim 6.5\%$ to $\sim 95.5\%$ with increasing

pH from 3 to 6, and then decreased with increasing pH at pH > 6. The sorption percent of UO_2^{2+} on raw MWCNT increased slowly with increasing pH from 4 to 6, then the sorption of UO_2^{2+} increased sharply with increasing pH from ~6 to ~6.8, and at last the sorption decreased with increasing pH at pH > 6.8.

Similar sorption behaviors of UO_2^{2+} on montmorillonite were reported by Hyun et al.^{4a} and Kowal-Fouchard et al.,^{4b} which was ascribed to the different U(VI) species in solution at different pH values and at different U(VI) concentrations. The sorption property of U(VI) as a function of pH value was corresponded to the change of U(VI) species with varying of pH values. As can be seen from Figure SI-3, U(VI) mainly exists as UO_2^{2+} at pH < 5, and then mainly exists as U(VI) hydrolysis complexes and multinuclear hydroxide complexes. Furthermore, U(VI) species are positively charged in pH range of ~5-8, and are negatively charged at pH > 8.

As can be seen from Figure SI-4, the maximum sorption percent of U(VI) by **MWCNT-g-CMC** is ~95.5% at pH ~6.0 (i.e., $C_{\text{eq}} = 9.0 \times 10^{-6}$ mol/L). From Figure SI-3C, U(VI) presents mainly as the specie of $(\text{UO}_2)_3(\text{OH})_5^+$ at pH 6-7 in 1.00×10^{-5} mol/L solution. The maximum sorption percent (~80.7%, $C_{\text{eq}} = 3.9 \times 10^{-5}$ mol/L) of U(VI) by raw MWCNT is found at pH ~6.8. From Figure SI-3B, $(\text{UO}_2)_3(\text{OH})_5^+$ and $(\text{UO}_2)_4(\text{OH})_7^+$ are the dominate species in 4.00×10^{-5} mol/L U(VI) solution at pH range of 5-8. The relative proportion of $(\text{UO}_2)_3(\text{OH})_5^+$ specie decreases with increasing pH at pH range of 6.0-8, whereas the relative proportion of $(\text{UO}_2)_3(\text{OH})_7^-$ increases with increasing pH at pH range of 7-9. Therefore, the result that the increase sorption of UO_2^{2+} on raw MWCNT and on **MWCNT-g-CMC** with increasing pH at pH < 6 can be

attributed to the species of UO_2^{2+} and $(\text{UO}_2)_3(\text{OH})_5^+$; whereas the decrease sorption of UO_2^{2+} with increasing pH at high pH values is due to the decreases of relative proportion of $(\text{UO}_2)_3(\text{OH})_5^+$ specie and the increase of the relative proportion of $(\text{UO}_2)_3(\text{OH})_7^-$ specie.

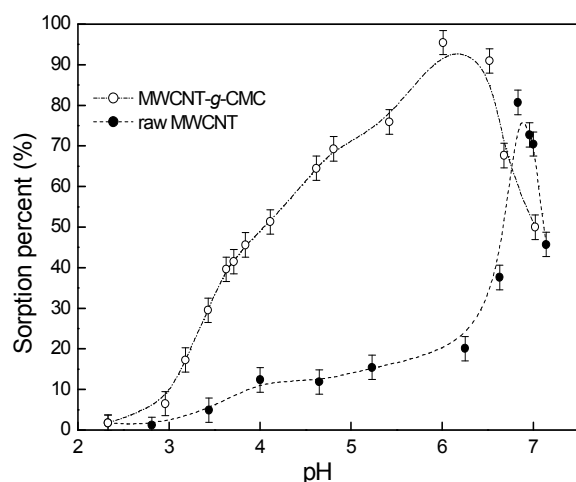


Figure SI-4. Sorption of UO_2^{2+} on raw MWCNT and on **MWCNT-g-CMC** as a function of pH values. $T = 25 \pm 2$ °C, equilibrium time 24 h, $C[\text{UO}_2^{2+}]_{(\text{initial})} = 2.00 \times 10^{-4}$ mol/L, $m/V = 0.40$ g/L, $C[\text{NaClO}_4] = 1.00 \times 10^{-2}$ mol/L.

SI-9. Effect of ionic strength on sorption of UO_2^{2+} on **MWCNT-g-CMC**

The effect of ionic strength on the sorption of UO_2^{2+} on **MWCNT-g-CMC** was shown in Figure SI-5. As can be seen from Figure SI-5, the sorption of UO_2^{2+} decreased with increasing ionic strength at low NaClO_4 concentrations. At $\text{pH} = 5.0 \pm 0.1$, the sorption percent of UO_2^{2+} decreased from ~83% to ~67% with increasing NaClO_4 concentrations from 1.0×10^{-3} mol/L to 5.0×10^{-2} mol/L, and then decreased slowly with increasing ionic strength. At $\text{pH} = 4.0 \pm 0.1$, the sorption percent of UO_2^{2+} decreased from ~62% to ~53% with increasing NaClO_4 concentrations from 1.0×10^{-3}

mol/L to 1.0×10^{-2} mol/L, and then the sorption percent of UO_2^{2+} did not decrease with increasing ionic strength. From the results in Figure SI-5, the sorption of UO_2^{2+} on **MWCNT-g-CMC** was influenced by ionic strength at low NaClO_4 concentrations, but was independent of ionic strength at high NaClO_4 concentrations. The results are very interesting. In wastewater, the salt concentration may be different. The independent ionic strength sorption of UO_2^{2+} on **MWCNT-g-CMC** at high salt concentrations is critical for the evaluation of **MWCNT-g-CMC** in wastewater cleaning management.

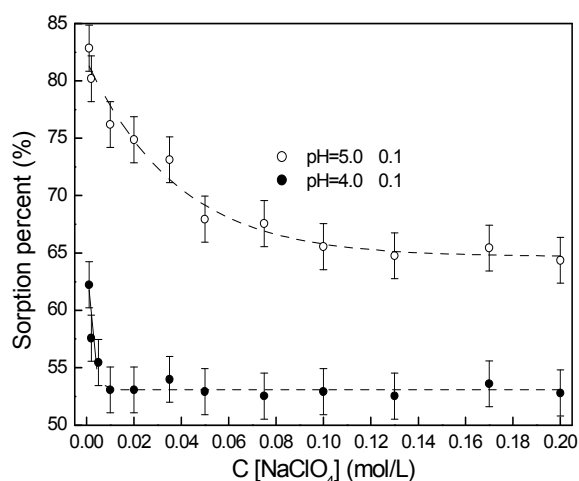


Figure SI-5. Sorption of UO_2^{2+} on **MWCNT-g-CMC** as a function of ionic strength. $T = 25 \pm 2$ °C, equilibrium time 24 h, $C[\text{UO}_2^{2+}]_{(\text{initial})} = 2.00 \times 10^{-4}$ mol/L, $m/V = 0.40$ g/L.

SI-10. Reference cited.

1. Wang, X.; Chen, C.; Hu, W.; Ding, A.; Xu, D.; Zhou, X. *Environ. Sci. Technol.* **2005**, *39*, 2856-2860.
2. (a) Vicini, S.; Princi, E.; Luciano, G.; Franceschi, E.; Pedemonte, E.; Oldak, D.; Kaczmarek, H.; Sionkowska, A. *Thermochim. Acta* **2004**, *418*, 123-130. (b) Kim, U. J.; Kuga, S.; Wada, M.; Okano, T.; Kondo, T. *Biomacromolecules* **2000**, *1*,

488-492.

3. (a) Gorman-Lewis, D.; Burns, P. C.; Fein, J. B. *J. Chem. Thermodynamics* 2008, *40*, 335-352. (b) Gorman-Lewis, D.; Fein, J. B.; Burns, P. C.; Szymanowski, J. E.S.; Converse, J. *J. Chem. Thermodynamics* 2008, *40*, 980-990.
4. (a) Hyun, S. P.; Cho, Y. H.; Hahn, P. S.; Kim, S. J. *J. Radioanal. Nucl. Chem.* 2001, *250*, 55-62. (b) Kowal-Fouchard, A.; Drot, R.; Simoni, E.; Ehrhardt, J. *J. Environ. Sci. Technol.* 2004, *38*, 1399-1407.